

Aluminum and E-glass epoxy plates behavior subjected to shock loading

Imrose B. Muhit^{*1}, Mostofa N. Sakib^{2a} and Sheikh S. Ahmed^{3b}

¹School of Civil and Environmental Engineering, Chung-Ang University, Seoul, Korea

²Institute of Water and Flood Management, Bangladesh University of Engineering and Technology, Dhaka, Bangladesh

³Department of Civil Engineering, University of Asia Pacific, Dhaka, Bangladesh

(Received March 17, 2017, Revised June 6, 2017, Accepted June 26, 2017)

Abstract. The terrorist attacks and dangers by bomb blast have turned into an emerging issue throughout the world and the protection of the people and structures against terrorist acts depends on the prediction of the response of structures under blast and shock load. In this paper, behavior of aluminum and unidirectionally reinforced E-Glass Epoxy composite plates with and without focal circular holes subjected to shock loading has been identified. For isotropic and orthotropic plates (with and without holes) the classical normal mode approach has been utilized as a part of the processing of theoretical results. To obtain the accurate results, convergence of the results was considered and a number of modes were selected for plate with and without hole individually. Using a shock tube as a loading device, tests have been conducted to composite plates to verify the theoretical results. Moreover, peak dynamic strains, investigated by experiments are also compared with the theoretical values and deviation of the results are discussed accordingly. The strain-time histories are likewise indicated for a specific gauge area for aluminum and composite plates. Comparison of dynamic-amplification factors between the isotropic and the orthotropic plates with and without hole has been discussed.

Keywords: aluminum; blast; composite plate; dynamic-amplification factor, epoxy plate; isotropic plate; orthotropic plate; shock load; shock tube

1. Introduction

Dynamic response of structures corresponding to shock load has been a matter of research for the affluent amount of studies in the last decade (Ramajeyathilagam *et al.* 2000, Türkmen 2002, Upadhyay *et al.* 2011, Daniel and Dubey 2014, Hosseini *et al.* 2016). A large amount of data has been generated from analytical and experimental method in parametric form for the last 25 years. With the ever increasing demand of shock and blast protective structures, structural engineers have been in search for the best materials to cope up with the huge knock as the outcome of those loads.

*Corresponding author, Researcher, E-mail: ibmuhit@cau.ac.kr

^aResearch Associate, E-mail: sakib.sajon@gmail.com

^bFaculty Member, E-mail: sharifce05@gmail.com

Aerospace industry, aircraft and naval sectors are the most vulnerable areas due to shock loads resulting from bombing in war, nuclear explosion and blasting of fuel (Türkmen 2002). Hence, these sectors are always in the continuing demand of shock enduring burly structures for both vulnerability assessment and sustainability (Ramajeyathilagam *et al.* 2000). The composite structure is proved to be more effective against the loads compared to its metallic counterpart as it can provide good resistance to creep, high stiffness and long fatigue life (Shim *et al.* 2001, Shim *et al.* 2012, Mazek and Wahab 2015).

Several researches are available on composite material structures with response to dynamic load. Most of those research works are based on the dynamic response of shell structures and isotropic plate subjected to blast loading (Houlston *et al.* 1985, Gupta *et al.* 1987, Houlston and Desrochers 1987, Olson 1991, Wiernicki *et al.* 1991, Redekop and Azar 1991) and materials on impact loading (Carvalho and Soares 1996, Aslan *et al.* 2002, Uyaner and Kara 2007, Yun *et al.* 2014). Very recently, stress-strain analysis and analytical approach for buckling (along with thermal buckling) of functionally graded plates and FGM nanoplates subjected to various load has been evaluated (Dhiraj *et al.* 2016, Daouadji and Adim 2016, Ancy and Parvathy 2016, Daouadji *et al.* 2016, Abdelhak *et al.* 2015, Hebali *et al.* 2016, Ebrahimi *et al.* 2016). Nonlinear damped vibration of a laminated composite with response to blast load has been studied by Kazanci and Mecitoglu (2006). Librescu and Nosier (1990) recorded high impact response of flat panels while facing extensive blast loading. Reddy (1983) checked laminated composite materials nonlinear response at the moment of undergoing large amount of deformation which account for inertia, shear strains and rotational force. Dynamic response of composite materials with respect to blast load was studied and equations of motion for cylindrical laminated shells are evolved using the Love's theory (Türkmen 1998). Librescu *et al.* (2004) studied the difficulties in dynamic responding when disclosed to blast loading. Finite element model with respect to finite strip has been developed through analyzing cylindrical structures and stiffened plate (Olson 1991). Continuous series of solution is generated from blast load response corresponding to a shell panel, which has time variation described by Friedlander decay function (Redekop 1994). Dynamic response from an imperfect panel was predicated utilizing Lagrange's equation while the panel used was shallow (Louca *et al.* 1998).

Confined vapor gas explosions can impart far greater levels of damage than that of unconfined ones due to the higher over pressures generated (Sohn *et al.* 2014, Schleyer *et al.* 2012, Babaei *et al.* 2015), and hole in the or openings in the plate structure is an important concern. In the past, research on plates with openings (hole) drew very limited attention, but recently research (Langdon *et al.* 2010) on plates with small openings has been conducted. This research lacks in investigations to identify the effects of hole on the plate. Li *et al.* (2002) studied the explosion resistance of square plates with openings for venting dust explosions for applications in the process industry.

For the blast and impact resistant panel design, aluminum plate (isotropic) and composite plate (orthotropic) are widely used. Therefore, the aim of this research is to evaluate the effectiveness and performance comparison of the aluminum and composite plate which enables to execute the economical and efficient protective structure design. From the literature there is no evidence of the experimental and mathematical approach for aluminum and glass epoxy plate with and without hole under shock loading. Based on this research gap, this study includes theoretical and experimental investigations of isotropic and orthotropic rectangular plate with and without hole. In a long chamber, shock tube plate was clamped and experimental investigation has been conducted. Utilizing modal analysis approach, theoretical results have been developed and convergence

studies have been carried out to obtain accurate results. Comparison of dynamic strain of the aluminum plates and unidirectionally reinforced E-glass epoxy plates at different strain gauge locations has been evaluated. Moreover, dynamic amplification factors (DAF) have been computed and discussed for both aluminum and composite plates with and without central hole.

2. Hypothetical equations

Considering geometrical discontinuities in the presence of external forces, the dynamic equations for composite plate are given as (Rajamani and Prabhakaran 1977a, 1977b, 1980)

$$\sum_{m=1}^R \sum_{n=1}^S (M_{mn}^{ij} - \beta_{mn}^{ij}) \ddot{q}_{mn} + \sum_{m=1}^R \sum_{n=1}^S (C_{mn}^{ij} - \alpha_{mn}^{ij}) q_{mn} = P_{Fij} \quad (1)$$

Where,

m = mode number in the x direction

n = mode number in the y direction

$R = a/b$, number of modes taken in the x direction

a = dimension of the plate in the x direction

b = dimension of the plate in the y direction

S = number of terms taken in the y direction

M_{mn}^{ij} = mass coefficients

$\alpha_{mn}^{ij}, \beta_{mn}^{ij}$ = stiffness and mass coefficients due to a hole

q_{mn} = generalized displacement coordinate in the mn mode

C_{mn}^{ij} = stiffness coefficients

P_{Fij} = generalized force

The expressions for $M_{mn}^{ij}, \beta_{mn}^{ij}, C_{mn}^{ij}, \alpha_{mn}^{ij}$, and P_{Fij} are

$$M_{mn}^{ij} = \int_0^a \int_0^b \rho h \Phi_{ij} \Phi_{mn} dA \quad (2)$$

$$\beta_{mn}^{ij} = \sum_{N_H} \int_{A_H} \rho h \Phi_{ij} \Phi_{mn} dA \quad (3)$$

$$C_{mn}^{ij} = \int_0^a \int_0^b [D_{11} \Phi_{ij,xx} \Phi_{mn,xx} + D_{12} (\Phi_{ij,xx} \Phi_{mn,yy} + \Phi_{ij,yy} \Phi_{mn,xx}) + D_{22} \Phi_{ij,yy} \Phi_{mn,yy} + 4D_{66} \Phi_{mn,xy} \Phi_{ij,xy} + 2D_{16} (\Phi_{mn,xx} \Phi_{ij,xy} + \Phi_{ij,xx} \Phi_{mn,xy}) + 2D_{26} (\Phi_{mn,yy} \Phi_{ij,xy} + \Phi_{mn,xy} \Phi_{ij,yy})] dA \quad (4)$$

$$\alpha_{mn}^{ij} = \sum_{N_H} \int_{A_H} [D_{11} \Phi_{ij,xx} \Phi_{mn,xx} + D_{12} (\Phi_{ij,xx} \Phi_{mn,yy} + \Phi_{ij,yy} \Phi_{mn,xx}) + D_{22} \Phi_{ij,yy} \Phi_{mn,yy} + 4D_{66} \Phi_{mn,xy} \Phi_{ij,xy} + 2D_{16} (\Phi_{mn,xx} \Phi_{ij,xy} + \Phi_{ij,xx} \Phi_{mn,xy}) + 2D_{26} (\Phi_{mn,yy} \Phi_{ij,xy} + \Phi_{mn,xy} \Phi_{ij,yy})] dA \quad (5)$$

$$P_{Fij} = \int \int_A F(x, y, t) \Phi_{i,j} dA \quad (6)$$

Where,

h = thickness of the plate

Φ_{mn} = admissible functions

A = effective area of the plate = $ab - N_H A_H$

N_H = number of holes

A_H = area of the hole

D_{ij} = elements of the plate bending stiffness matrix

$F(x, y, t)$ = external dynamic load

To evaluate the coefficients M_{mn}^{ij} , β_{mn}^{ij} , C_{mn}^{ij} , and α_{mn}^{ij} , only one hole has been considered. Moreover, in x and y directions it is assumed that $\Phi_{mn}(x, y)$ is a product of beam characteristic functions. To evaluate the coefficients M_{mn}^{ij} and C_{mn}^{ij} , definite integrals are necessary and these can be obtained in close form. On the contrary, numerical integration scheme is needed to identify the definite integrals which are necessary for determining β_{mn}^{ij} and α_{mn}^{ij} because these integrals cannot be found in closed form. Therefore, for this purpose a sixteen-point Gauss quadrature formula has been used. If Eq. (1) is expressed as a matrix form

$$[\bar{M}]\{\ddot{\bar{q}}\} + [\bar{K}]\{\bar{q}\} = \{\bar{P}\} \quad (7)$$

Where,

$$\bar{M} = M_{mn}^{ij} - \beta_{mn}^{ij}$$

$$\bar{K} = C_{mn}^{ij} - \alpha_{mn}^{ij} = \text{modified stiffness matrix coefficients}$$

$$\bar{P} = P_{Fij} q = q_{mn}$$

$$P = (i - 1)S + j$$

Numerically, an arrangement of second order linear differential equations is indicated by Eq. (7). Furthermore, differential mathematical equations with consistent coefficients can be solved by standard methodology. But if matrix order is large and equations are coupled, this methodology or procedure can be more complex. For solving Eq. (7), Bathe and Wilson (1986) introduced direct integration and classical normal mode methods. Due to availability of results from a free vibration, normal mode approach has been used in this study with neglecting the damping condition.

By following uncoupled differential equations transformation from generalized coordinates to normal mode generalized coordinates can be done.

$$\ddot{\eta}_r(t) + \omega_r^2 \eta_r(t) = N_r(t); \quad r = 1, 2, \dots, n \quad (8)$$

With the initial conditions

$$\eta_r(0) = \{\bar{A}\}_r^T [\bar{M}] \{\bar{q}(0)\} \quad (9)$$

$$\dot{\eta}_r(0) = \{\bar{A}\}_r^T [\bar{M}] \{\dot{\bar{q}}(0)\} \quad (10)$$

Where,

$\{\bar{A}\}$ = eigen vector

The solution of Eq. (8) can be re-written as following by applying Laplace transformation

$$\eta_r(t) = \eta_r(0) \cos \omega_r t + \dot{\eta}_r(0) \frac{\sin \omega_r t}{\omega_r} + \frac{1}{\omega_r} \int_0^t N_r(t) \sin \omega_r (t - c) dt \quad (11)$$

$$r = 1, 2, \dots, n$$

Where,

$\eta_r(t)$ = modal generation coordinate

t = time variable

For a shock wave advancing through any physically real barotropic medium, the nature of the reflected wave is uniquely determined by the relative shock impedance of the medium through which the incident wave passes and the medium upon which it falls (Pack 1957). More discussions about properties of shock wave have been reported by Dewey (2001) and Needham (2012).

At the end of the shock tube the composite plate was located and subjected to plane shock wave assuming unit magnitude with distributed load which is shown in Fig. 1.

$$F(t) = 0 \quad -\infty < t < 0 \text{ and } t > t_2 \quad (12)$$

$$= 1 \quad t < t_1 \quad (13)$$

$$= 1 - \frac{t - t_1}{t_2 - t_1} \quad t_1 \leq t \leq t_2 \quad (14)$$

Where,

t_1, t_2 = time parameters defining the shock load

Modal generalized force, $N_r(t)$ can be developed from following relation and Eq. (11) can be solved by $N_r(t)$.

$$N_r(t) = [\bar{A}]_r^T \int \int_A F(x, y, t) \Phi_{ij} dA \quad (15)$$

By inverse transformation, the generalized coordinates $q_{mn}(t)$ can be found after modal generalized coordinates calculation $\eta_r(t)$ from Eq. (11) have been done. From the following expressions, obtained from Bathe and Wilson (1986), displacements and strains can be determined

$$\omega(x, y, t) = \sum_{m=1}^R \sum_{n=1}^S q_{mn}(t) \Phi_{mn}(x, y) \quad (16)$$

$$\varepsilon_x(x, y, t) = -\frac{h}{2} \sum_{m=1}^R \sum_{n=1}^S q_{mn}(t) \frac{\delta^2 \Phi_{mn}(x, y)}{\delta x^2} \quad (17)$$

$$\varepsilon_y(x, y, t) = -\frac{h}{2} \sum_{m=1}^R \sum_{n=1}^S q_{mn}(t) \frac{\delta^2 \Phi_{mn}(x, y)}{\delta y^2} \quad (18)$$

3. Experimental program

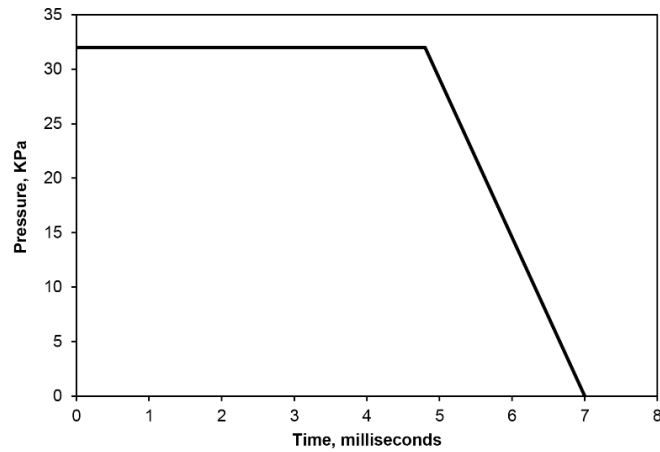


Fig. 1 Pressure-time histories (idealized)

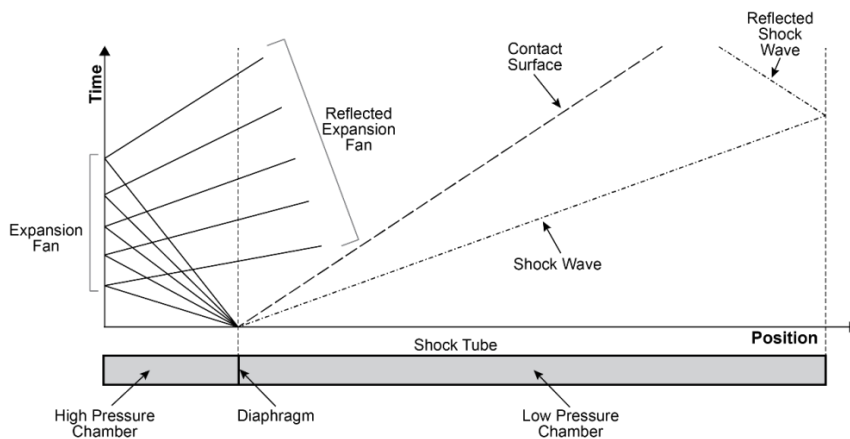


Fig. 2 An idealized shock tube

The experimental approach for identifying the behavior of aluminum and E-glass epoxy Plates subjected to shock loading can be divided into three categories:

- (a) The shock tube
- (b) Evaluation of Pressure-Time variation
- (c) Aluminum and composite plates for shock testing

To replicate the blast waves and shock loads in a small scale, a long chamber shock tube with a constant cross section of 150 mm×100 mm was used for this study. It is separated at two pressure chambers through a diaphragm based on the pressure difference namely high pressure and low pressure chamber. An idealized shock tube is shown in Fig. 2 which depicted the formation of different waves in the tube once the diaphragm is burst. The high pressure chamber has a length of 1000 mm while low pressure chamber has five separate sections 700 mm long each. The different sections on the low pressure side are joined by means of flanges and made air tight with rubber gaskets provided at the junctions. The chambers are connected through a circular flange joint with provision for two O-rings. An inlet valve and a pressure gauge were introduced on the high pressure side. Shock wave is produced at the high pressure chamber by supplying compressed air

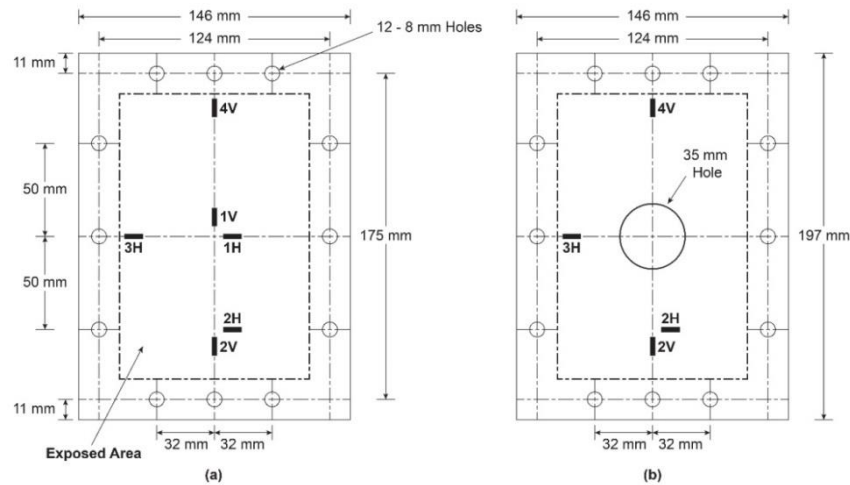


Fig. 3 Dimension and strain gauge locations of the test plates (a) without (b) with hole

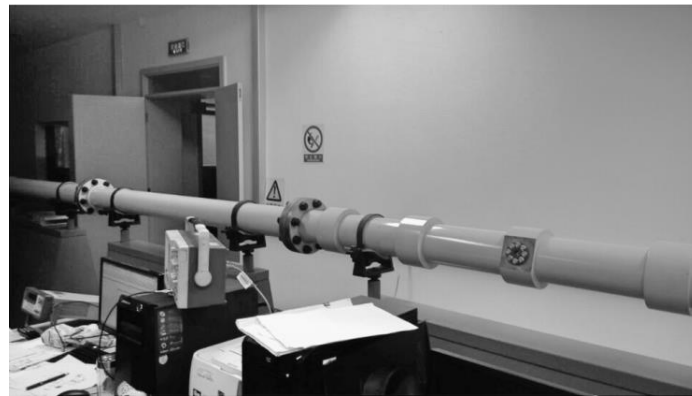


Fig. 4 Part of the Experimental setup

from the compressor. The center of the diaphragm is pierced through which a wire is passed to carry high current for the formulation of shock wave.

Since the pressure-time variation of shock wave requires to be measured to compare its result with computed values, two piezoelectric pressure transducers were used to measure the pressure. One was mounted at the low pressure end on shock tube and another was attached at the end of shock tube on stiff plate. Pressure data are collected from the transducers and both of those had an identical pressure variation and peak pressure. To identify whether the shock wave was plane or not, two pressure transducers were mounted at two arbitrary points on a stiff plate to record pressure-time history. This history was recorded on dual-beam storage oscilloscope which proved that shock wave traveling to the end of shock tube was plane.

In the current study, aluminum plates of 1.2 mm thickness were prepared from Aluminum Alloy 2024 which has very high strength to weight ratio and good fatigue resistance. It has a density of 2.78 g/cm^3 , Young's modulus of 73 GPa and Poisson's ratio of 0.3, which were used for calculation. On the other hand, thickness of 2.4 mm reinforced E-glass epoxy composite plates were fabricated using simple hand lay-up technique where glass fibers (20% of volume) were

Table 1 Elastic modulus properties for the reinforced E-glass epoxy composite plate

Properties	Static value	Dynamic value
Young's modulus in the major material symmetry-axis direction (E_{11})	14 GPa	14.5 GPa
Young's modulus in the minor material symmetry-axis direction (E_{22})	3.5 GPa	4.9 GPa
Principal shear modulus (G_{12})	1.4 GPa	2.0 GPa
Major Poisson's ratio (ν_{12})		0.3

Table 2 Dynamic responses of aluminum plate without hole based on number of modes

No. of Modes	Deflection (mm)	Strain					
		1H	2H	3H	1V	2V	4V
3	0.638274	410.25	280.14	-419.19	202.62	101.73	-255.39
5	0.600192	398.11	289.38	-398.85	162.88	136.89	-278.90
7	0.589128	389.79	285.66	-393.33	151.67	142.32	-275.76
9	0.573433	383.88	279.56	-392.16	149.81	143.28	-274.38
11	0.574254	384.13	279.62	-392.23	149.93	143.52	-274.84

Table 3 Dynamic responses of aluminum plate with hole based on number of modes

No. of Modes	Strain			
	2H	3H	2V	4V
9	326.78	-439.22	102.22	-245.33
11	329.23	-433.23	119.89	-218.11
13	329.98	-431.78	130.98	-201.56
15	330.21	-430.97	131.98	-193.22
17	330.13	-430.87	132.33	-194.43

placed layer by layer (up to required thickness) and liquid epoxy (with hardener) were applied on the fibers. These layers formed a solid polymer after curing for 24 hours in ambient conditions. Through forced vibration response method (Shabana 1996) and material characterization, dynamic and static properties of the composite materials were evaluated respectively. Elastic modulus properties of composite materials are shown in Table 1. For both aluminum plates (isotropic) and composite plates (anisotropic) without and with holes (35 mm diameter) were used for this study. Strain gauge were mounted horizontally (width of the plate) and vertically (length of the plate) to measure the dynamic strain. However, all the plates were attached at the end of the shock tube by bolt connection for testing. The positioning of the strain gauges and dimension of both test plates are shown at Fig. 3. A picture of the experimental setup is shown in Fig. 4.

The pressure-time history was obtained by piezoelectric pressure transducers corresponding to each strain measurement and was normalized with pressure.

4. Convergence studies

Convergence of the results is necessary to obtain accurate results from theoretical

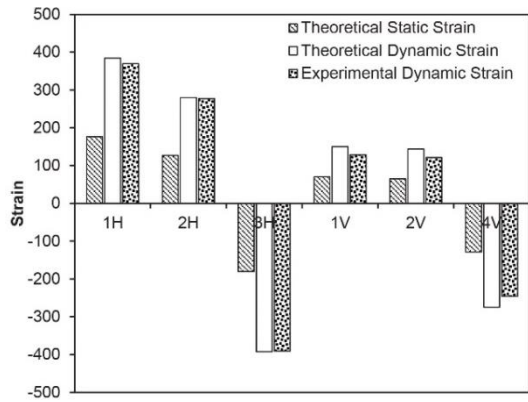


Fig. 5 Theoretical and experimental strains comparison for aluminum plate without hole

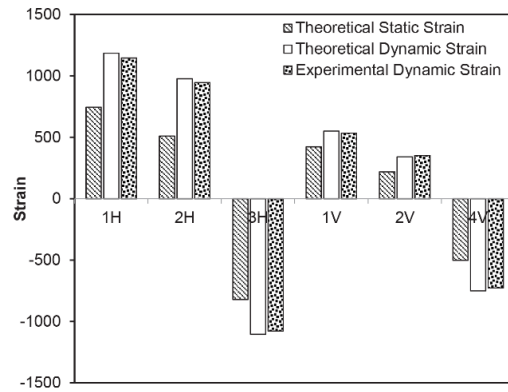


Fig. 6 Theoretical and experimental strains comparison for unidirectionally reinforced E-glass epoxy plate without hole

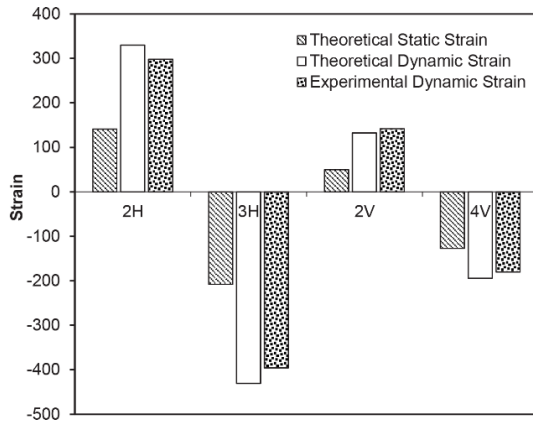


Fig. 7 Theoretical and experimental strains comparison for aluminum plate with hole

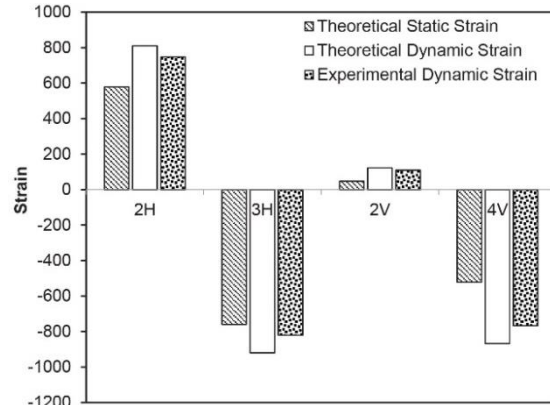


Fig. 8 Theoretical and experimental strains comparison for unidirectionally reinforced E-glass epoxy plate with hole

considerations. Number of modes taken into consideration for numerical investigations are the prerequisite to get convergence of the results. At first, considering different number of modes deflection and dynamic strain were calculated for isotropic plate (aluminum) without hole which is shown in Table 2. However, it is evident that with the increase of mode numbers, the results are going to merge and finally for eleven modes satisfactory convergence is achieved. That is why to compute theoretical results eleven modes were considered for all isotropic plate without hole. Moreover, for the orthotropic plate (composite) the necessity of higher number of modes is more important and eleven modes provide satisfactory convergence. Research (Kalnins and Dym 1976, Moradipour *et al.* 2015, Wang *et al.* 2016) shows that, modal method is perfectly suitable for the spatial load distribution on the entire smooth plate. On the contrary, the number of required modes would be increased if there is an abrupt discrepancy in the spatial load distribution. To overcome this difficulty, plates with hole were considered for higher number of modes to model the abrupt discrepancy (hole) of the plate and convergence studies are shown in Table 3. Dynamic strains of both isotropic and orthotropic plates with holes were calculated considering seventeen modes instead of eleven, where eleven nodes may not give the acceptable results.

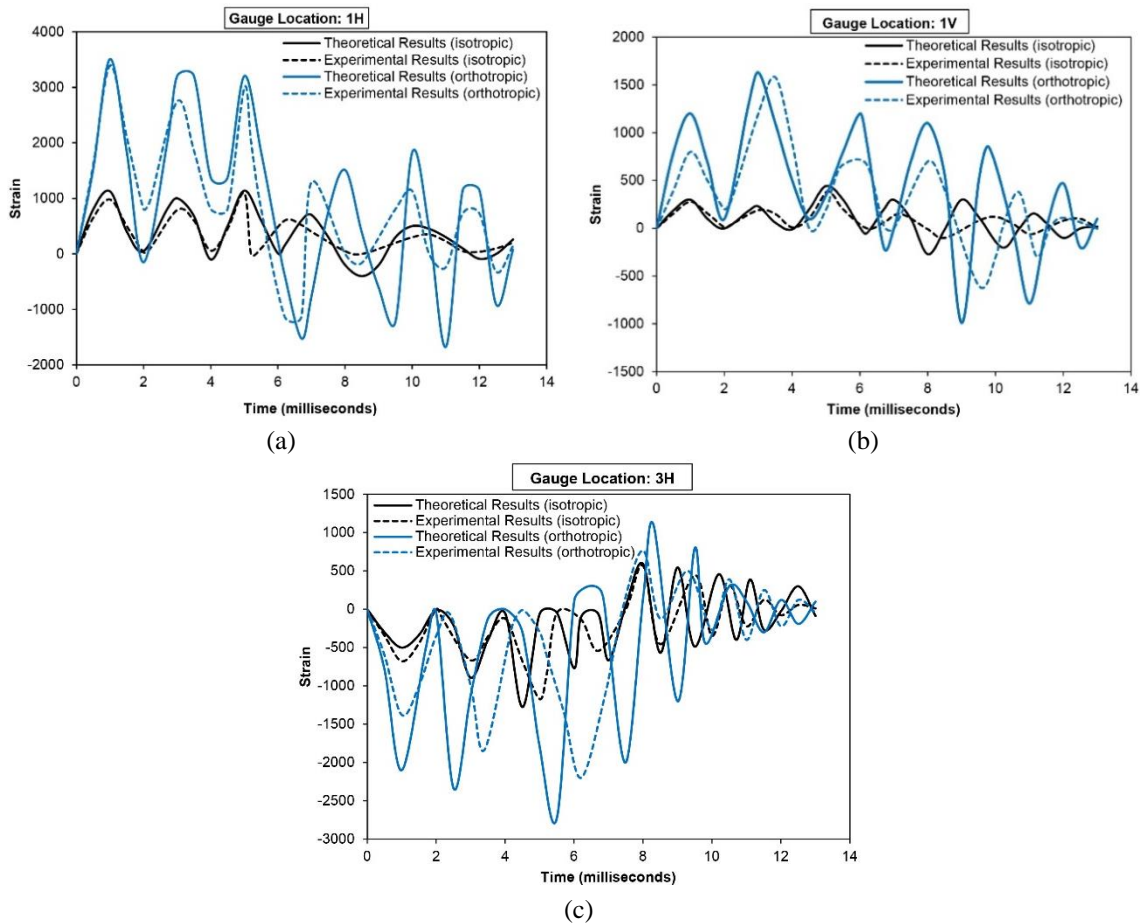


Fig. 9 Theoretical and experimental strain-time histories of isotropic and orthotropic plates (a) and (b) without hole, and (c) with hole

5. Results and discussion

Peak strains (static and dynamic) computed from theory and peak dynamic strains recorded from the experiments are normalized with maximum pressure for aluminum and unidirectionally reinforced E-glass epoxy composite plates. Theoretical and experimental results are compared to verify the experimental investigations for both types of plates with and without hole.

Fig. 5 illustrates the theoretical and experimental comparison of strains at different gauge locations for aluminum plate without hole and it shows decent agreement. Maximum strains were observed along the central width (1H and 3H) of the plate. Similarly, the experimental dynamic peak strains of composite plate without hole are comparable to strain values obtained theoretically shown in Fig. 6. But it is important to mention that the differences of results (theoretical and experimental strain values) between isotropic and orthotropic plates (without hole) are higher for composite plates than those of aluminum plates. This is because of the anisotropy of the material which may need a higher number of modes along the width of the plate. Similar differences of results for isotropic and orthotropic plates were observed by Dhiraj (2016), Rajamani (1980), and

Table 4 Theoretical DAF for aluminum and E-glass epoxy plates without and with hole

Gauge Location	Theoretical DAF			
	Aluminum plate		Unidirectionally reinforced E-glass epoxy plate	
	Without hole	With hole	Without hole	With hole
1H	2.18	-	1.59	-
2H	2.20	2.34	1.91	1.40
3H	2.18	2.07	1.35	1.21
1V	2.14	-	1.31	-
2V	2.20	2.64	1.56	2.61
4V	2.13	1.53	1.49	1.66

Ramajeyathilagam (2000). Some suitable analytical approach with software simulation could have been useful to get better results.

Apart from that, minor variances can be seen from the comparison results of the aluminum plate with a hole which is indicated in Fig. 7. However, the differences are less than 10%, and can be accepted for this study. On the contrary, for the case of unidirectionally reinforced E-glass epoxy composite plates with central circular holes, the agreement of theoretical and experimental strain values is considered not satisfactory as shown in Fig. 8. The divergence of the results exceeds 10% which might be due to the slight non-compatibility of modal method in spatial load distribution where sharp variations occur due to central hole. As the deviation of the computed value is not larger, it is not advisable to negate the modal approach for the plate with abrupt discrepancy rather it can be suggested that suitable mathematical modification for consideration of hole can increase the accuracy of this approach.

Figs. 9(a) and 9(b) represent the theoretical and experimental comparison of strain-time variations for both isotropic (aluminum) and orthotropic (E-glass epoxy composite) plates without holes on strain gauge location 1H and 1V, respectively. In addition, Fig. 9(c) represents the theoretical and experimental comparison of strain-time variations for both isotropic (aluminum) and orthotropic (E-glass epoxy composite) plates with hole on strain gauge location 3H. From the figures it is evident that, the experimental results followed the trend of theoretical results with satisfactory agreements which validate the experimentally computed strains for the given pressure pulse duration. Kumari (2017), Liou (1996) and Upadhyay (2011) reported that, the strain time history would be symmetric about zero line after the load is removed (from the duration obtained from pressure-time history). In this study, as per pressure time history the duration was 7 ms and from Fig. 9 it can be seen that, the pulses are symmetric about x -axis after 7 ms.

The ratio of the theoretical peak dynamic strain to the static strain can be defined as the theoretical dynamic amplification factor (DAF). Table 4 tabulates the DAFs of both aluminum and unidirectionally reinforced E-glass epoxy composite plate with and without hole. The DAFs for the solid aluminum plate lies between 2.1 and 2.2 whereas the DAF fluctuates from 1.3 to 1.9 for the solid composite plate. It is to be mentioned here that DAF values between 2 and 2.5 for isotropic aluminum plate and, between 1.3 and 1.8 for orthotropic composite plate under blast loading were suggested by Rajamani (1980). Apart from that, there is no disparity observed for the DAFs of the plate with hole compare to those without (solid) hole. But at 2V strain gauge location, the DAF increases significantly especially for the composite plate. Due to the presence of the hole,

the static strain was significantly minimized at 2V strain gauge location without affecting dynamic strain which resulted the increase of the DAF on that location.

6. Conclusions

In this study, both theoretical and experimental investigations have been performed to evaluate the behavior of aluminum and E-glass epoxy plates with and without hole under shock loading. The experimental results have been compared with the theoretical results obtained utilizing modal analysis approach. The following conclusions can be drawn from the present study:

- For the aluminum plate without hole, a good agreement between the theoretical and experimental results is observed.
- In the case of the composite plate without hole, the differences in results obtained by theory and experiment are higher than those of the aluminum plate because of the anisotropy of the composite plate.
- The dynamic amplification factors (DAFs) for the solid aluminum plate lie between 2.1 and 2.2, whereas those for solid composite plate vary between 1.3 and 1.9.
- The DAF values for the plate with hole compare well to those for the solid plate except for the strain-gauge location 2V where the static strain is minimized because of the presence of hole without affecting the dynamic strain. The decrease in static strain thus increases the DAF on that location. It should be mentioned here that the DAF value is noteworthy to calculate the dynamic load generated from blast and impact subjected to structures which is too significant to design the blast resistant structures (UFC 2008).
- The fairly good comparison between the theoretical and experimental results shows that the modal analysis approach can be used as a strong tool to evaluate the behavior of both aluminum and E-glass epoxy plates with and without hole under blast load.

References

- Abdelhak, Z., Hadji, L., Daouadji, T. and Bedia, E. (2015), "Thermal buckling of functionally graded plates using an-order four variable refined theory", *Adv. Mater. Res.*, **4**(1), 31-44.
- Ancy, A. and Parvathy, U. (2016), "Thermal buckling behaviour of functionally graded plates", *Appl. Mech. Mater.*, **857**, 279-284.
- Aslan, Z., Karakuzu, R. and Sayman, O. (2002), "Dynamic characteristics of laminated woven E-glass-epoxy composite plates subjected to low velocity heavy mass impact", *J. Compos. Mater.*, **36**(21), 2421-2442.
- Bathe, K.J. and Wilson, E.L. (1986), *Numerical Methods in Finite Element Analysis*, Englewood Cliffs, Prentice-Hall.
- Carvalho, A. and Soares, C.G. (1996), "Dynamic response of rectangular plates of composite materials subjected to impact loads", *Compos. Struct.*, **34**(1), 55-63.
- Daniel, A.J. and Dubey, R.N. (2015), "Finite element simulation of earthquake resistant brick masonry building under shock loading", *Adv. Struct. Eng.*, 1027-1038.
- Daouadji, T.H. and Adim, B. (2016), "An analytical approach for buckling of functionally graded plates", *Adv. Mater. Res.*, **5**(3), 141-169.
- Daouadji, T.H., Benferhat, R. and Adim, B. (2016), "A novel higher order shear deformation theory based on the neutral surface concept of FGM plate under transverse load", *Adv. Mater. Res.*, **5**(2), 107-120.
- Dewey, J.M. (2001), *Expanding Spherical Shocks (Blast Waves)*, Handbook of Shock Waves, Academic

- Press, Burlington, 441-481.
- Dhiraj, V.S., Jadvani, N. and Kalita, K. (2016), "Stress and strain analysis of functionally graded plates with circular cutout", *Adv. Mater. Res.*, **5**(2), 81-92.
- Ebrahimi, F., Ehyaei, J. and Babaei, R. (2016), "Thermal buckling of FGM nanoplates subjected to linear and nonlinear varying loads on Pasternak foundation", *Adv. Mater. Res.*, **5**(4), 245-261.
- Gupta, A.D., Gregory, F.H., Bitting, R.L. and Bhattacharya, S. (1987), "Dynamic analysis of an explosively loaded hinged rectangular plate", *Comput. Struct.*, **26**(1-2), 339-344.
- Hebali, H., Bakora, A., Tounsi, A. and Kaci, A. (2016), "A novel four variable refined plate theory for bending, buckling, and vibration of functionally graded plates", *Steel Compos. Struct.*, **22**(3), 473-495.
- Hosseini, S.A., Abolbashari, M.H. and Hosseini, S.M. (2016), "Generalized coupled non-Fickian/non-Fourierian diffusion-thermoelasticity analysis subjected to shock loading using analytical method", *Struct. Eng. Mech.*, **60**(3), 529-545.
- Houlston, R. and Desrochers, C.G. (1987), "Nonlinear structural response of ship panels subjected to air blast loading", *Comput. Struct.*, **26**(1-2), 1-15.
- Houlston, R., Slater, J.E., Pegg, N. and Desrochers, C.G. (1985), "On analysis of structural response of ship panels subjected to air blast loading", *Comput. Struct.*, **21**(1-2), 273-289.
- Kalnins, A. and Dym, C.L. (1976), *Vibration: Beams, Plates, and Shells*, Stroudsburg, Dowden, Hutchinson & Ross.
- Kazanci, Z. and Mecitoglu, Z. (2006), "Nonlinear damped vibrations of a laminated composite plate subjected to blast load", *AIAA J.*, **44**(9), 2002-2008.
- Kumari, E. and Singha, M. (2017), "Nonlinear response of laminated panels under blast load", *Proc. Eng.*, **173**, 539-546.
- Librescu, L. and Nosier, A. (1990), "Response of laminated composite flat panels to sonic boom and explosive blast loadings" *AIAA J.*, **28**(2), 345-352.
- Librescu, L., Oh, S.Y. and Hohe, J. (2004), "Linear and non-linear dynamic response of sandwich panels to blast loading", *Compos. Part B: Eng.*, **35**(6-8), 673-683.
- Liou, W., Tseng, C. and Chao, L. (1996), "Stress analysis of laminated E-glass epoxy composite plates subject to impact dynamic loading", *Comput. Struct.*, **61**(1), 1-11.
- Louca, L.A., Pan, Y.G. and Harding, J.E. (1998), "Response of stiffened and unstiffened plates subjected to blast loading", *Eng. Struct.*, **20**(12), 1079-1086.
- Mazek, S.A. and Wahab, M.M. (2015), "Impact of composite materials on buried structures performance against blast wave", *Struct. Eng. Mech.*, **53**(3), 589-605.
- Moradipour, P., Chan, T.H. and Gallag, C. (2015), "An improved modal strain energy method for structural damage detection, 2D simulation", *Struct. Eng. Mech.*, **54**(1), 105-119.
- Needham, C.E. (2012), *Blast Waves*, Springer-Verlag Berlin and Heidelberg GmbH & Co. KG, Berlin, Germany.
- Olson, M.D. (1991), "Efficient modelling of blast loaded stiffened plate and cylindrical shell structures", *Comput. Struct.*, **40**(5), 1139-1149.
- Pack, D.C. (1957), "The reflection and transmission of shock waves I: The reflection of a detonation wave at a boundary", *Philosoph. Mag.*, **2**(14), 182-188.
- Rajamani, A. and Prabhakaran, R. (1977a), "Dynamic response of composite plates with cut-outs, part I: Simply-supported plates", *J. Sound Vibr.*, **54**(4), 549-564.
- Rajamani, A. and Prabhakaran, R. (1977b), "Dynamic response of composite plates with cut-outs, part II: Clamped-clamped plates", *J. Sound Vibr.*, **54**(4), 565-576.
- Rajamani, A. and Prabhakaran, R. (1980), "Response of composite plates to blast loading", *Exper. Mech.*, **20**(7), 245-250.
- Ramajeyathilagam, K., Vendhan, C.P. and Rao, V.B. (2000), "Non-linear transient dynamic response of rectangular plates under shock loading", *J. Imp. Eng.*, **24**(10), 999-1015.
- Reddy, J.N. (1983), "Geometrically nonlinear transient analysis of laminated composite plates", *AIAA J.*, **21**(4), 621-629.
- Redekop, D. (1994), "Dynamic response of a toroidal shell panel to blast loading", *Comput. Struct.*, **51**(3),

- 235-239.
- Redekop, D. and Azar, P. (1991), "Dynamic response of a cylindrical shell panel to explosive loading", *J. Vibr. Acoust.*, **113**(3), 273-278.
- Shabana, A.A. (1996), *Forced Vibration, Theory of Vibration: An Introduction*, Springer, New York, U.S.A.
- Shim, C., Lee, P. and Chang, S. (2001), "Design of shear connection in composite steel and concrete bridges with precast decks", *J. Constr. Steel Res.*, **57**(3), 203-219.
- Shim, C., Yun, N., Yu, R. and Byun, D. (2012), "Mitigation of blast effects on protective structures by aluminum foam panels", *Metal.*, **2**(2), 170-177.
- Türkmen, H.S. (1998), "Dynamic response of laminated composite panels subjected to blast loading", Ph.D. Dissertation, Istanbul Technical University.
- Türkmen, H.S. (2002), "Structural response of laminated composite shells subjected to blast loading: Comparison of experimental and theoretical methods", *J. Sound Vibr.*, **249**(4), 663-678.
- UFC (2008), *Structures to Resist the Effects of Accidental Explosions*, Unified Facilities Criteria, United States Army, US Government Printing Office, Washington, U.S.A.
- Upadhyay, A.K., Pandey, R. and Shukla, K.K. (2011), "Nonlinear dynamic response of laminated composite plates subjected to pulse loading", *Commun. Nonlin. Sci. Numer. Simulat.*, **16**(11), 4530-4544.
- Uyaner, M. and Kara, M. (2007), "Dynamic response of laminated composites subjected to low-velocity impact", *J. Compos. Mater.*, **41**(24), 2877-2896.
- Wang, Y., Xu, C., Wan, Y., Li, J., Yu, H. and Ren, L. (2016), "A modal approach for the efficient analysis of a bionic multi-layer sound absorption structure", *Steel Compos. Struct.*, **21**(2), 249-266.
- Wiernicki, C.J., Liem, F., Woods, G.D. and Furio, A.J. (1991), "Structural analysis methods for lightweight metallic corrugated core sandwich panels subjected to blast loads", *Naval Eng. J.*, **103**(3), 192-202.
- Yun, N.R., Park, S.D., Muhit, I.B. and Shim, C.S. (2014), "Impact tests on aluminum foams", *Proceedings of the 4th International Technical Conference*, Seoul, Korea, November.